Baseline and longitudinal variability of normal tissue uptake values of [F-18]-fluorothymidine-PET images

Cysouw, Matthijs C. F.; Kramer, Gerbrand M.; Frings, Virginie; De Langen, Adrianus J.; Wondergem, Marielle J.; Kenny, Laura M.; Aboagye, Eric O.; Kobe, Carsten; Wolff, Juergen; Hoekstra, Otto S.

Published in:
Nuclear Medicine and Biology

DOI:
10.1016/j.nucmedbio.2017.05.002

Publication date:
2017

Nuclear Medicine and Biology 51 (2017) 18–24

Contents lists available at ScienceDirect

Nuclear Medicine and Biology

journal homepage: www.elsevier.com/locate/nucmedbio

Baseline and longitudinal variability of normal tissue uptake values of [^{18}F]-fluorothymidine-PET images

Matthijs C.F. Cysouw [a,*], Gerbrand M. Kramer [a], Virginie Frings [a], Adrianus J. De Langen [b], Mariëlle J. Wondergem [c], Laura M. Kenny [d], Eric O. Aboagye [d], Carsten Kobe [e], Jürgen Wolf [f], Otto S. Hoekstra [a], Ronald Boellaard [a,g]

[a] Department of Radiology & Nuclear Medicine, VU University Medical Center, Amsterdam, The Netherlands
[b] Department of Pulmonary diseases, VU University Medical Center, Amsterdam, The Netherlands
[c] Department of Hematology, VU University Medical Center, Amsterdam, The Netherlands
[d] Imperial College London, and Hammersmith Hospital NHS Trust, London, UK
[e] Department of Nuclear Medicine, Center for Integrated Oncology Köln Bonn, University Hospital of Cologne, Cologne, Germany
[f] Department I of Internal Medicine, Center for Integrated Oncology Köln Bonn, University Hospital of Cologne, Cologne, Germany
[g] Nuclear Medicine & Molecular Imaging, University of Groningen, University Medical Center Groningen, Groningen, The Netherlands

ARTICLE INFO

Article history:
Received 22 February 2017
Received in revised form 14 April 2017
Accepted 4 May 2017

Keywords:
^{18}F–FLT
PET
Normal tissue uptake values
Quality control

ABSTRACT

Purpose: [^{18}F]-fluorothymidine ([^{18}F]-FLT) is a PET-tracer enabling in-vivo visualization and quantification of tumor cell proliferation. For qualitative and quantitative analysis, adequate knowledge of normal tissue uptake is indispensable. This study aimed to quantitatively investigate baseline tracer uptake of blood pool, lung, liver and bone marrow and their precision, and to assess the longitudinal effect of systemic treatment on biodistribution.

Methods: ^{18}F–FLT-PET(/CT) scans (dynamic or static) of 90 treatment-naïve oncological patients were retrospectively evaluated. Twenty-three patients received double baseline scans, and another 39 patients were also scanned early and late during systemic treatment with a tyrosine kinase inhibitor. Reproducible volume of interest were placed in blood pool, lung, liver, and bone marrow. For semi-quantitative analysis, SUVmean, SUVmax, and SUVpeak with several normalizations were derived.

Results: SUVs of basal lung, liver, and bone marrow were not significantly different between averaged dynamic and static images, in contrast with blood pool and apical lung. Highest repeatability was seen for liver and bone marrow, with repeatability coefficients of 18.6% and 20.4% when using SUVpeak. Systemic treatment with TKIs both increased and decreased normal tissue tracer uptake at early and late time points during treatment.

Conclusion: Simultaneous evaluation of liver and bone marrow uptake in longitudinal response studies may be used to assess image quality, where changes in uptake outside repeatability limits should trigger investigators to perform additional quality control on individual PET images.

Advances in knowledge: For [^{18}F]-FLT PET images, liver and bone marrow have low intra-patient variability when quantified with SUVpeak, but may be affected by systemic treatment.

Implications for patient care: In [^{18}F]-FLT-PET response monitoring trials, liver and bone marrow uptake may be used for quality control of [^{18}F]-FLT PET images.

1. Introduction

[^{18}F]-fluorothymidine ([^{18}F]-FLT) is an [^{18}F]-bound thymidine analogue enabling visualization and quantification of tumor cell proliferation using positron emission tomography (PET) [1,2]. In contrast with [^{18}F]-fluorodeoxyglucose ([^{18}F]-FDG), inflammatory processes are less of an issue for [^{18}F]-FLT [3]. Previous research investigating [^{18}F]-FLT uptake as biomarker of response to treatment has proven it to be a useful tracer for assessing or predicting progression-free and disease-free survival for several types of cancer [4].

In oncological PET(/CT) studies, normal tissue uptake can be used both qualitatively and quantitatively to assess malignancy of suspected lesions. Typically, a lesion is considered malignant if tracer uptake exceeds background uptake of surrounding tissue in qualitative visual analysis. In addition, uptake values of reference tissues such as blood or liver are used to normalize tumor uptake in semi-quantitative

* Corresponding author at: Department of Radiology and Nuclear Medicine, VU University Medical Center, 7057, 1007MB Amsterdam, Netherlands. Tel.: +31 20 4444214.
E-mail address: m.cysouw@vumc.nl (M.C.F. Cysouw).

http://dx.doi.org/10.1016/j.nucmedbio.2017.05.002

analysis, generating a tumor-to-background ratio (TBR). However, when variability of uptake in normal tissues within patients is high, TBR may become an unreliable parameter reflecting true tumor activity rather poorly and obscuring discriminative value of quantitative PET.

Simplified measures, such as standardized uptake values (SUV) and TBR have proven useful for response assessment using [^{18}F]-FLT-PET/CT [5]. However, to use SUV reliably one needs to control for technical image flaws, such as mistakes made in injected activity [6]. Additionally, in order to use these simplified methods during treatment, biodistribution and pharmacokinetics may not change drastically over time. Hence, an image quality control method is necessary to allow for appropriate quantification of tumor activity.

Much research has been performed into normal tissue uptake and its intra-patient variability in [^{18}F]-FDG-PET [7–10]. However, as the biodistribution of [^{18}F]-FLT is inherently different to that of [^{18}F]-FDG, results from these studies cannot merely be assumed to be applicable to [^{18}F]-FLT-PET studies. As [^{18}F]-FLT is establishing itself as a valuable oncological PET-tracer, researchers and physicians should have knowledge of its normal tissue uptake variability within and between patients.

In this study we aimed at deriving normal [^{18}F]-FLT uptake values and their precisions for several tissues and/or organs and to explore if these could be used to assess image quality for individual scans and/or longitudinally. As [^{18}F]-FLT is often used in lung cancer patients, we assessed the effect of tyrosine-kinase inhibitor (TKI) treatment on normal tissue uptake values in lung cancer patients. Tissues investigated were lung, blood pool, liver, and bone marrow. Several SUV types were investigated, with several volumes of distribution normalizations.

2. Materials and methods

2.1. Patients

Images of 90 patients scanned with [^{18}F]-FLT-PET(/CT) at baseline (i.e. while receiving no systemic treatment), were gathered from six single-center study cohorts and investigated in a retrospective analysis. One cohort of 28 patients with non-Hodgkin lymphoma (NHL) consisted only of baseline scans [11]. Twenty-three out of 90 patients received double baseline scans in order to assess intra-patient variability, with head and neck cancer (n = 6), non-small cell lung cancer (NSCLC; n = 9), and breast cancer (n = 8), [12,13]. In two cohorts of patients with NSCLC, a total of 39 patients were, in addition to the baseline scans, also scanned early (after approximately 1 week) and late (one cohort after 4 and one cohort after 6 weeks) during treatment with a TKI [5,14]. A description of the included study cohorts is provided in Table 1. All included studies were approved by the medical ethical committee of the respective research institutes and patients gave informed consent for participation.

2.2. Image acquisition

For extensive descriptions of image acquisition methods we refer to the included studies' primary publications. Reconstruction methods and scanning modes (i.e. dynamic and static) with acquisition times (post injection) are summarized in Table 1. Static scanning was performed approximately 60 min post-injection of [^{18}F]-FLT. Frames of dynamic scans were averaged over 45–60 min, 45–65 min, and 50–60 min, depending on available frame durations, to generate comparable static images allowing evaluation of effect of uptake intervals on SUVs.

2.3. Quantitative image analysis

Volumes of interest (VOI) of fixed size and shape were placed in lung, liver, bone marrow, and ascending aorta. Within the lung, uptake may be a function of variation in perfusion, air density, liver spill-in, and diaphragmatic motion. Therefore, we placed 3 cm diameter spheres apically as well as basally. For blood pool, a VOI 2 or 4 voxels (depending on voxel size) in diameter with an axial length of 2 cm was placed in the ascending aorta, which was identified on low-dose CT or on dynamic PET-images acquired shortly after injection of ^{18}F–FLT. In six patients with head and neck cancer the aorta was outside the field of view, in which case the left carotid artery was used. In liver, a 3 cm diameter sphere was placed in the upper right lobe. Vertebrae were used to quantify bone marrow uptake; both single and multiple (3) lower thoracic vertebrae were delineated using circular VOIs (5 or 9 voxels, depending on voxel size), avoiding the vertebral cortex. Tissues with known or apparent disease were avoided.

From each VOI, SUVmean (mean SUV within the VOI), SUVmax (maximum SUV value within the VOI), and SUVpeak (mean SUV within a 12 mm diameter sphere positioned within the VOI to yield the highest value) were extracted. SUV was calculated according to the following equation:

$$\mathrm{SUV} = [\mathrm{AC}/(\mathrm{ID}/\text{normalization factor})], \quad (1)$$

where AC = activity concentration (Bq/mL), ID = injected dose at time of scanning (Bq). Normalization factors were bodyweight (BW; kilogram), lean body mass (LBM; kilogram), and body surface area (BSA; m^2). The latter two were calculated according to the following equations:

$$\mathrm{LBM_{male}} = 1.10^{*}\text{weight}\text{-}128.0^{*}(\text{weight}/\text{height})^2 \quad (2)$$

$$\mathrm{LBM_{female}} = 1.07^{*}\text{weight}\text{-}148.0^{*}(\text{weight}/\text{height})^2 \quad (3)$$

$$\mathrm{BSA} = 0.007184^{*}\text{weight}^{0.425*}\text{height}^{0.725} \quad (4)$$

Normalization factors were indicated as suffix to SUV (e.g. SUVpeak-bw, being the peak SUV normalized to bodyweight).

2.4. Statistical analysis

For baseline SUVs, mean with standard deviation (SD) was calculated for (averaged) dynamic and static data, to illustrate SUVs as a function of acquisition time. In addition, coefficients of variation (COV%) were calculated to describe variability of uptake values. Shapiro–Wilks test was used to assess normality of data. For data with skewed distribution, data were log-transformed for statistical analysis. To assess differences between dynamic and static data for each SUV

Table 1
Description of included cohorts. Frames of dynamic acquired images were averaged.

Ref	Study type	No. patients	Cohort	Reconstruction	Scanner	Acquisition	Uptake interval
[11]	Baseline	28	NHL	BLOB-OS-TF	PET/CT	Static	60 min
[14]	Treatment	30	NSCLC	OSEM	PET	Static	60 min
[12]	Repeatability	6	HNC	OSEM	PET	Dynamic	45–60 min
[12]	Repeatability	9	NSCLC	OSEM	PET	Dynamic	45–60 min
[5]	Treatment	9	NSCLC	RAMLA	PET/CT	Dynamic	50–60 min
[13]	Repeatability	8	BC	FBP	PET	Dynamic	45–65 min

NHL = non-Hodgkin lymphoma; NSCLC = non-small cell lung cancer; HNC = head-and-neck cancer; BC = breast cancer; OSEM = ordered subset expectation maximization; BLOB-OS-TF = iterative time-of-flight reconstruction; RAMLA = row-action maximum likelihood algorithm; FBP = filtered back projection.

type, first Levene's test was used to assess equality of variances. Next, an independent samples t-test was applied to investigate differences between the two samples. Additionally, we calculate reference ranges using 5th–95th percentiles. Extreme outliers (<[Q_1–3*IQR] or >[Q_3 + 3*IQR]) were censored for calculation of reference ranges. The effect of age and gender on baseline uptake values were analyzed using multivariate linear regression.

To investigate repeatability (i.e. intra-patient variability), repeatability coefficients (RC) were calculated. Relative differences and RCs were calculated as follows:

$$\text{Relative difference} = (\text{scan2-scan1})/[(\text{scan1} + \text{scan2})/2)]^{*}\ 100 \quad (5)$$

$$\text{RC} = 1.96^{*}\ \text{SD}, \quad (6)$$

where the SD is taken from the relative differences.

To illustrate the effect of treatment on normal tissue uptake, relative change of SUV was calculated using the following formula:

$$\text{Relative change} = [(\text{scan2-scan1})/\text{scan 1}]^{*}\ 100 \quad (7)$$

Relative changes were described using mean ± SD. All statistical analyses were performed using IBM SPSS v22.0 (Armonk, USA).

3. Results

3.1. Baseline uptake values

Baseline scans were categorized into two groups to investigate tissue uptake as function of uptake interval; one group consisted of dynamic images (frames averaged 45/50 to 60/65 min p.i.) and one group of static images (60 min p.i.).

The effects of age and gender on uptake values were analyzed in multivariate analysis, while correcting for acquisition type (static or dynamic). Age was only a significant modifier for lung SUVmax-bw ($p = 0.035$–0.046). Gender was a significant modifier for all SUV types of bone marrow (single vertebra), liver, and blood pool when using LBM for normalization ($p = 0.003$–0.046). For bone marrow (multiple vertebrae), gender was a modifier for SUVmean-LBM ($p = 0.029$). For lung, gender was a modifier for SUVmean-bsa and SUVpeak-bsa ($p = 0.013$–0.026).

Henceforth, the remainder of the paper will focus on results of SUVpeak normalized to bodyweight. All other data can be found in the supplemental data.

Table 2 contains average SUVpeak-bw, of all investigated tissues (Supplemental Table 1 for SUVmean and SUVmax). No extreme outliers were identified. Blood pool and apical lung SUVpeak were significantly different between averaged dynamic and static images ($p = 0.001$ and $p = 0.041$, respectively). In contrast, SUVpeak of basal lung, liver, and bone marrow were not significantly different between dynamic and static images, for all normalization factors ($p = 0.604$, $p = 0.126$, and $p = 0.444$–0.592, respectively). For bone marrow using multiple vertebrae, only SUVmax was significantly different between dynamic and static images, regardless of normalization factor ($p = 0.027$–0.049).

The distribution of SUVpeak (COV%) is illustrated in Fig. 1 as a function of dynamic and static images. COVs of blood pool and bone marrow between static and dynamic images were similar within 1%. For apical and basal lung, COVs between dynamic and static images were −8.8% and 1.7% different, respectively. For liver, COVs between dynamic and static images were −10.8% different.

To further illustrate the differences in SUV between the averaged dynamic and static images, time-activity curves of mean uptake in the investigated tissues are displayed in Fig. 2 for a dynamic scan of a typical patient. A gradual decrease in activity concentrations can be seen for blood pool and lung. Notably, the time-activity curve of lung tissue has a very similar shape to the blood pool curve, suggesting that it is mainly blood pool which is measured in lung. A decrease in liver activity is noted over time, which corresponds to the data in Table 2. Bone marrow seems to be increasing at 55 min p.i., but it could have reached a plateau at 60 min p.i. since there were no significant differences in bone marrow SUVmean between averaged dynamic and static images.

Before defining reference ranges for SUVs of whole-body static scans (60 min p.i.), differences in SUVs between the static PET and PET/CT cohort were investigated. For liver and bone marrow, significant differences were found for SUVmean and SUVpeak (all normalizations; $p = 0.000$–0.024), but not for SUVmax. For lung, significant differences were found for SUVmax (all normalizations; $p = 0.000$–0.005), but not for SUVmean and SUVpeak. For blood pool, only PET/CT data were available for the static scans. As differences in SUV between PET and PET/CT static whole-body scans were observed, reference ranges were calculated for the hybrid PET/CT cohort only. Reference ranges for SUVpeak-bw (Supplemental Table 2 for other SUVs) of whole body static PET/CT scans 60 min post-injection were 0.44–1.04 for blood pool, 0.34–0.83 for lung (apical), 3.46–7.46 for liver, and 4.86–11.36 for bone marrow (multiple vertebrae).

3.2. Repeatability

Intra-patient variability of normal tissue SUVs between double baseline scans was investigated using RCs. There were no significant dissimilarities between the normalizations of each SUV, with differences in RCs between normalizations ranging 0.03–0.80%. For all SUV types, liver and bone marrow (multiple vertebrae) provided the lowest RCs.

Liver and bone marrow (multiple vertebrae) SUVpeak-bw RCs were 18.6% and 20.4%, respectively. Blood pool, lung (apical and basal), and bone marrow (single vertebrae) SUVpeak-bw RCs were 27.4%, 43.3%, 46.3%, and 24.3%, respectively (Supplemental Fig. 1 for other SUVs).

3.3. Longitudinal variability

Two cohorts of NSCLC patients were scanned at baseline, and early (approximately 1 week) and late (4 or 6 weeks, respectively) after starting treatment with TKIs. Since between the SUVs of late scans of the two cohorts (at 4 and 6 weeks) no significant differences in relative changes from baseline were found, these data were pooled together. For one cohort blood pool could not be evaluated due to absence of co-registered CT and early dynamic PET images [14]. In the other cohort liver could not be evaluated due to the chest only scan trajectory [5].

Table 3 contains the mean relative changes of SUVpeak-bw during systemic treatment (Supplemental Table 3 for SUVmean and SUVmax). Early during treatment the smallest relative changes were observed for blood pool (−1.24 ± 15.71%). In contrast, blood pool had the largest relative changes late during treatment (7.89 ± 17.63%). It should be

Table 2
Baseline SUVpeak-bw of blood pool, lung, liver, and bone marrow.

	Blood pool	Lung (apical)	Lung (basal)	Liver	Bone marrow (single)	Bone marrow (multiple)
Dynamic	0.87 ± 0.20	0.67 ± 0.28	0.60 ± 0.24	5.86 ± 2.15	6.42 ± 1.67	6.48 ± 1.69
Static	0.70 ± 0.17	0.55 ± 0.19	0.57 ± 0.24	4.76 ± 1.23	6.26 ± 1.70	6.80 ± 1.79
p-value	**0.001**	**0.041**	0.604	0.126	0.592	0.444

Data from averaged dynamic image frames and static images are displayed separately. Significant differences in bold.

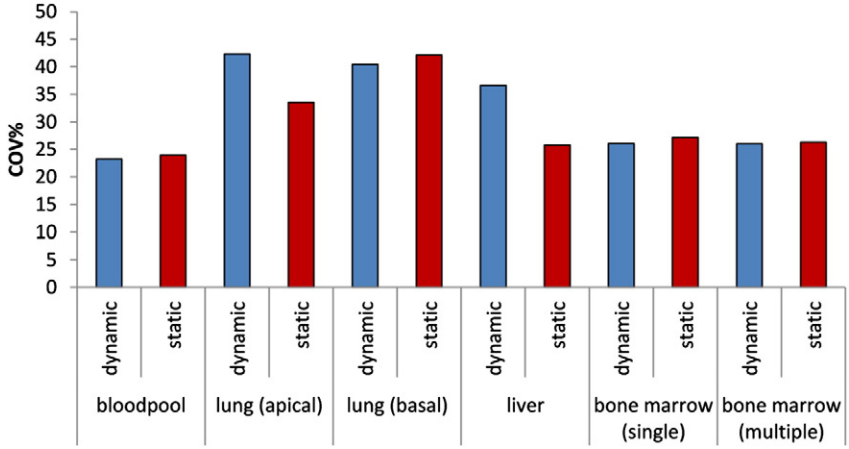

Fig. 1. Coefficients of variation (%) of SUVpeak-bw for all reference tissues determined on averaged dynamic and static images.

noted that even though the spread in relative changes was quite large, early during treatment all tissues except blood pool demonstrated mean increases in tracer uptake. Lung uptake increased most early during TKI treatment (7.2 ± 25.5% and 14.8 ± 35.0% for apical and basal lung, respectively), with the smallest relative changes late during treatment (−1.23 ± 27.87% and 2.19 ± 34.16% for apical and basal lung, respectively).

For further illustration, Fig. 3 exhibits relative changes of SUVs, respectively, from baseline for all individual patients, in which the large ranges of changes from baseline are clearly visible (Supplemental Fig. 2 for absolute changes). For each tissue, the SUV with optimal intra- and inter-patient variability is displayed. Fig. 4 illustrates images of two patients with aberrant increases in uptake (early

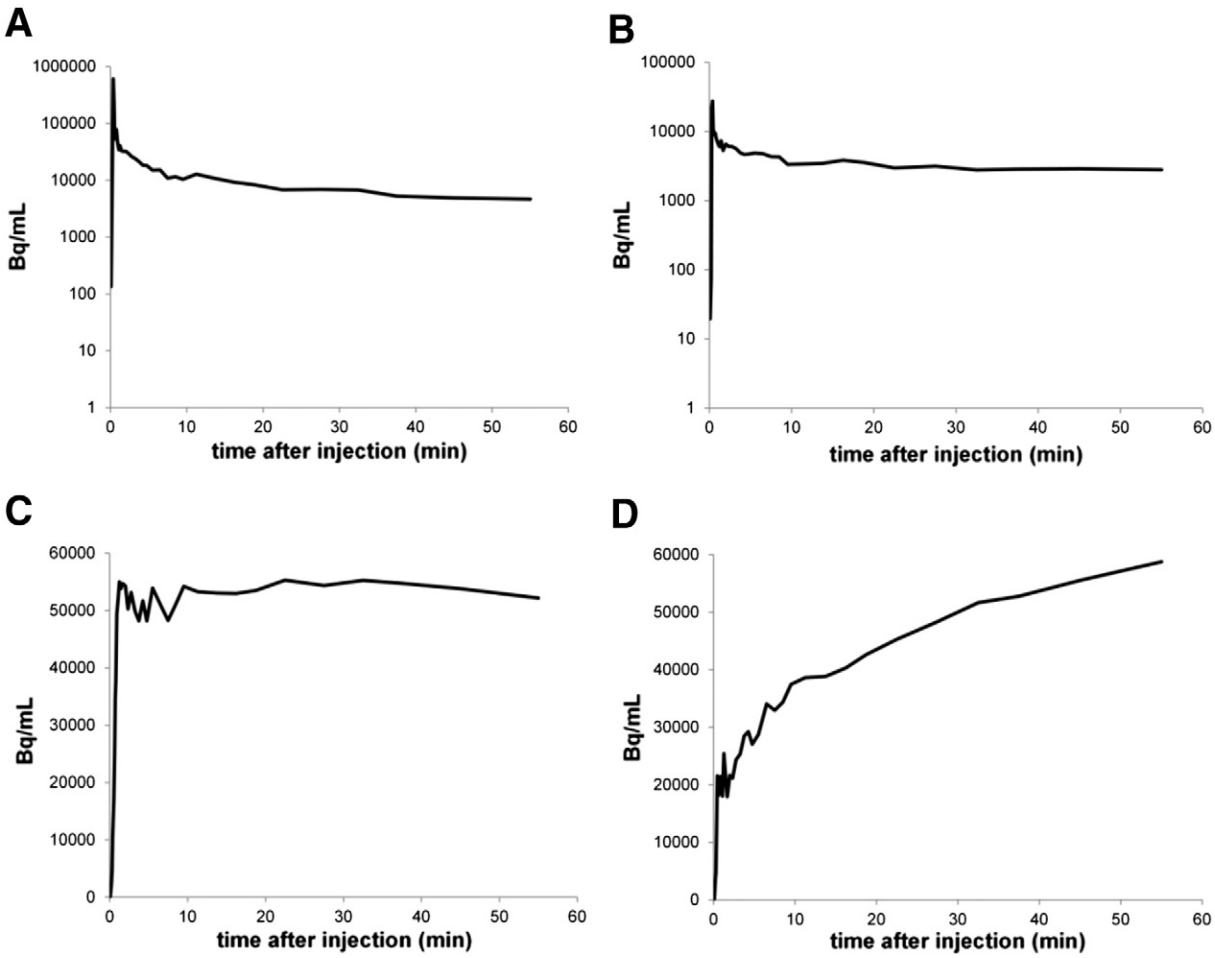

Fig. 2. Tissue time-activity curves for blood pool (A), lung (B), liver (C), and bone marrow (D). Curves are generated from dynamic images of a typical patient, in this case with NSCLC. Blood pool and lung curves are displayed with a logarithmic y-axis to enhance visual interpretation.

Table 3
Relative change from baseline of SUVpeak-bw of reference tissues early and late during treatment with TKIs.

	Blood pool	Lung (apical)	Lung (basal)	Liver	Bone marrow (single)	Bone marrow (multiple)
Early	−1.24 ± 15.71	7.19 ± 25.47	14.77 ± 35.04	7.26 ± 16.51	3.09 ± 18.07	3.82 ± 17.62
Late	7.89 ± 17.63	−1.23 ± 27.87	2.19 ± 34.16	6.13 ± 25.13	6.69 ± 29.93	7.24 ± 29.50

Results are relative changes (mean ± SD) from baseline, in percentages.

during treatment) in lung (+209%) and bone marrow (+67%), respectively. Remarkably, these patients only demonstrated these aberrant increases in one tissue type.

4. Discussion

[^{18}F]-FLT is a PET tracer increasingly used in oncological response assessment PET(/CT)-studies, providing a biomarker of tumor proliferation for several types of cancer, such as NSCLC, head and neck squamous cell carcinoma, and breast cancer [4]. The aims of this paper on normal reference tissue uptake values of [^{18}F]-FLT-PET(/CT) images were to evaluate their inter- and intra-patient variability, and to assess the longitudinal variability of these values during systemic treatment with TKIs. In addition to the most commonly used reference tissues, being liver and blood pool, we also investigated lung and bone marrow uptake.

Knowledge of reference values of normal tissue is critical for qualitative image analysis, where malignancy is suspected if lesion uptake exceeds background uptake. Furthermore, in quantitative analysis a TBR may be used to distinguish between benign and malignant lesions and for measuring response to treatment. Additionally, reference tissue uptake may be used to calculate a threshold for malignancy, as done for [^{18}F]-FDG-PET in the PERCIST criteria using mean liver uptake [15]. Also, reliability of (semi-)quantitative analysis of tumor tracer uptake is affected by the technical quality with which a PET study is performed [16,17]. Hence, a reliable reference value with low inter-patient variability may serve as an image-based quality control method.

SUVmean, SUVmax, and SUVpeak have different characteristics regarding sensitivity to noise and inter- and intra-observer variability caused by VOI placement [18,19]. Most commonly, in clinical practice and clinical studies, SUVmax is used due to its low dependency on accurate and reliable VOI placement and hence ease of applicability. However, its sensitivity to noise level may render it an unreliable parameter of normal tissue tracer uptake, especially in multi-center studies. SUVpeak seems an appropriate alternative in this context, due to its intrinsically lower sensitivity to noise fluctuations and similarly low dependency on VOI placement. Lodge et al. found that for quantification of primary brain tumors SUVpeak indeed provided best repeatability at 60 min post-injection, making it an attractive SUV for tumor quantification [20]. In this study, however, while intra-patient variability was different between SUV types, conclusions regarding the most reliable tissues (liver and bone marrow) were similar regardless of SUV type.

Considering the intra-patient variability of normal tissue uptake in this study, liver seems to be the most stable reference tissue (Fig. 3). Remarkably, SUVmax demonstrated the lowest intra- and inter-patient variability for this tissue. However, SUVpeak had very

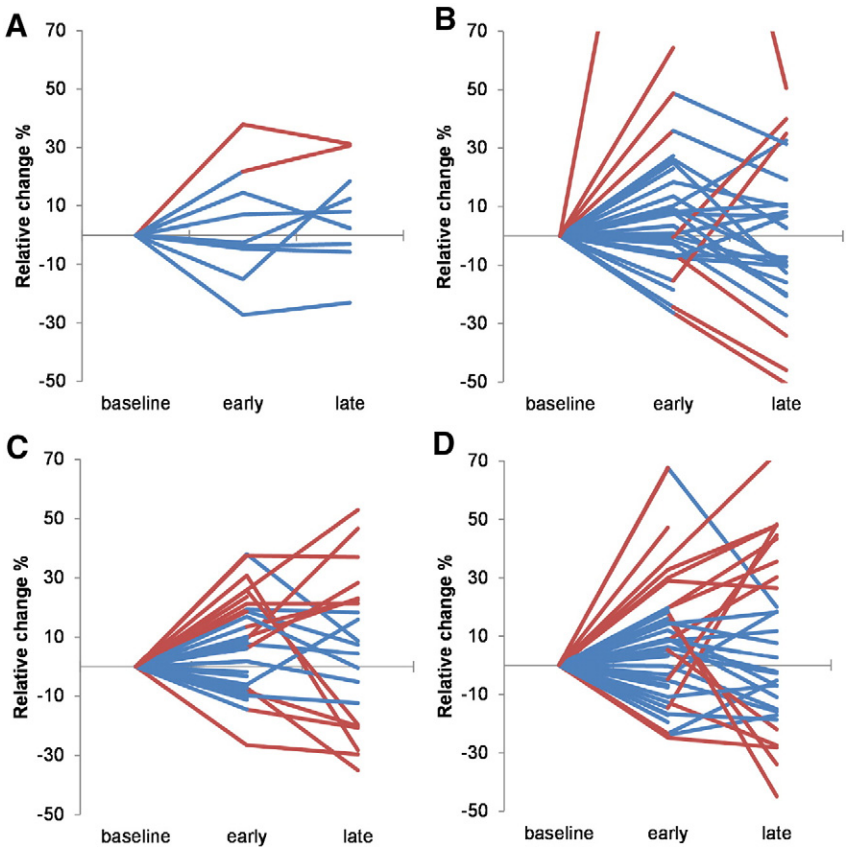

Fig. 3. Relative changes from baseline (%) early and late during treatment of NSCLC with TKIs of blood pool (A, SUVpeak), lung (B, SUVmean), liver (C, SUVpeak), and bone marrow (D, SUVpeak). Each line represents an individual patient. Blue and red lines indicate relative changes below and above repeatability coefficients (%), respectively, for the SUV with optimal repeatability determined per tissue type (Fig. 3). For a patient in (B) relative change in lung SUVmean of 209% exceeded the y-axis.

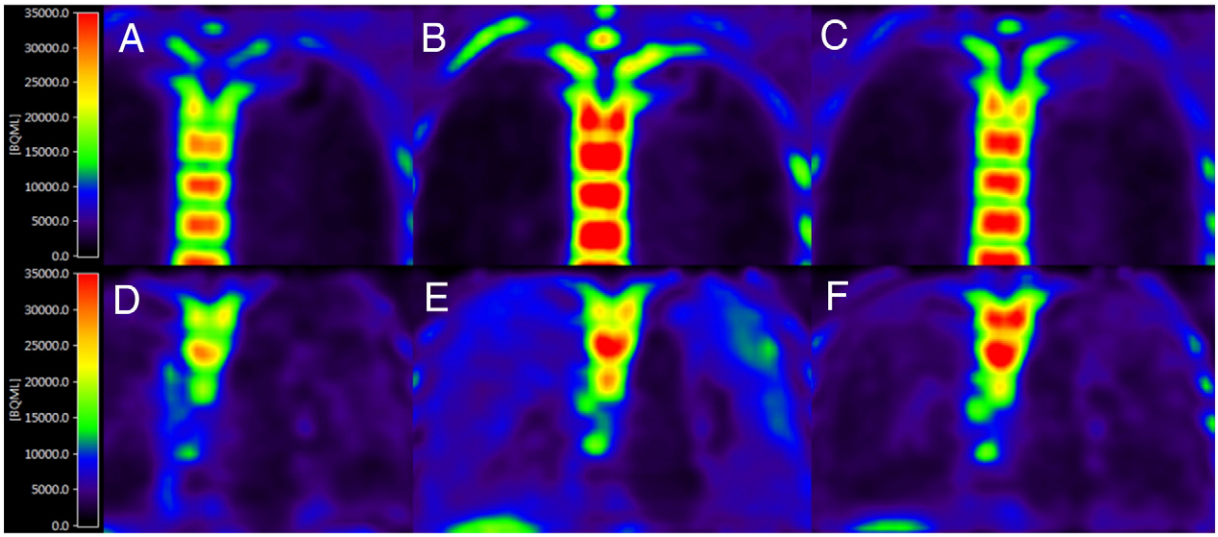

Fig. 4. Coronal ^{18}F–FLT-PET images of two NSCLC patients demonstrating substantial increases in tracer uptake in bone marrow (A–C) and lung (D–F), respectively, early after starting treatment with TKI. Images of baseline (A, D) and 1 week (B, E), and 4 weeks (C, F) after starting treatment. Images represent frames acquired at 50–60 min post-injection. Injected activities were: A, 397 MBq; B, 375 MBq; C, 395 MBq; D, 350 MBq; E, 366 MBq; F, 378 MBq.

similar repeatability and is preferred due to its lower sensitivity to image noise. The second lowest RCs were observed for bone marrow SUVpeak when derived from multiple vertebrae. Additionally, SUVpeak was not different between averaged dynamic and static images for both liver and bone marrow (Table 2). Blood pool and lung SUVs seemed less stable than liver and bone marrow, and these tissues should not be used as reference.

During treatment (with TKIs) we observed changes in biodistribution larger than test–retest limits (Fig. 3), which could be a consequence of altered tracer kinetics and/or metabolism during systemic treatments. Drugs affecting glucuronidation of FLT in liver or renal clearance of FLT may result in altered area-under-the-curves of the arterial input functions. Also, drugs affecting tissue proliferation (specifically bone marrow in this study) may explain these changes in FLT uptake. The observed treatment-induced alterations in FLT kinetics can explain why in previous research tumor-to-blood ratios seemed most appropriate for assessment of treatment response in locally advanced breast cancer and NSCLC, when correlated with full kinetic modeling [5,21]. A rationale for this is that tumor SUVs fluctuate with blood pool activity, and use of tumor-to-blood ratios may compensate for variations in arterial input functions. Overall, this emphasizes the importance of dynamic PET/CT validation studies before SUVs can be used for tumor quantification during treatment.

Taken together, we recommend liver and bone marrow to be used as normal tissue references for [^{18}F]-FLT-PET images. SUVpeak of these tissues demonstrated good repeatability and was not affected by differences in uptake intervals. Liver uptake can be easily quantified by placing a 3 cm diameter spherical VOI in the right upper liver lobe and measuring SUVpeak. For bone marrow quantification we suggest delineating three adjacent vertebrae, avoiding the vertebral cortex, and measuring SUVpeak. We observed no significant advantage of using either bodyweight, lean body mass, or body surface area for SUV normalization in this context. However, LBM and BSA may be affected by gender type, thus using bodyweight is preferred.

As both liver and bone marrow uptake can change during systematic treatment a conservative approach could be to assess liver and bone marrow and verify if these uptakes are within expected ranges and remain constant during treatment. If this would not be the case it does not necessarily imply poor image quality and/or poor execution of the PET/CT study, but it could alert the observer to perform additional quality control on the images such as verification of injected activities, uptake times and acquisition/reconstruction settings. Also it should alert the observer that there are changes in tracer uptake biodistribution that may affect lesion uptake interpretation as well. The changed biodistribution could namely also result from a change in arterial input function as was shown before for tumor quantification for [^{18}F]-FLT and [^{18}F]-FDG [5,22].

This study has several limitations, among which the heterogeneity between studies due to the retrospective nature. However, Kuhnert et al. found that while different reconstructions provide different SUVs for tumors, this was not the case for liver tissue [23]. This is probably due to the fact that differences in noise and contrast between reconstructions do not affect SUV of homogeneous tissue when using a mean uptake value, such as SUVmean or SUVpeak. Despite heterogeneity between cohorts we were able to identify liver and bone marrow as the most reliable reference tissues, with similar RCs as seen for tumor SUVs [13]. In addition, perhaps a smaller reference range for liver and bone marrow uptake can be determined in future studies performing commonly used PET acquisition modes for ^{18}F-FLT-PET images (i.e. static whole body scans performed 60 min after injection) with larger sample sizes.

5. Conclusion

We investigated blood pool, lung, liver, and bone marrow uptake of [^{18}F]-FLT -PET(/CT) images in oncological patients. Liver and bone marrow seemed most appropriate for image-based quality control due to high repeatability. However, clinicians should be aware of the variable susceptibility of normal tissue SUVs to physiologic treatment effects in patients undergoing systemic treatments. Simultaneous evaluation of liver and bone marrow uptake in longitudinal response studies may be used to assess image quality, where changes in SUVs outside repeatability limits should trigger investigators to perform additional quality control on individual PET images.

Compliance with ethical standards

Part of the research leading to these results has received support from the Innovative Medicines Initiative Joint Undertaking (www.imi.europa.eu; grant agreement number 115151), whose resources are composed of a financial contribution from the European Union's Seventh Framework Programme (FP7/2007-2013) and an in-kind contribution from the companies of the European Federation of Pharmaceutical Industries and Associations. Authors Cysouw, Kramer,

de Langen, Frings, Wondergem, Aboagye, Kenny, Kobe, Hoekstra, Boellaard declare no conflicts of interest. Author Wolf is on advisory boards (compensated) of, and receives lecture fees from AstraZeneca, BMS, Boehringer-Ingelheim, MSD, Clovis, Novartis, Pfizer, and Roche, and has received research support from Novartis, Pfizer, BMS, and MSD. All procedures performed in studies involving human participants were in accordance with the ethical standards of the institutional and/or national research committee and with the 1964 Helsinki declaration and its later amendments or comparable ethical standards.

Acknowledgment

The authors acknowledge the Quantitative Imaging in Cancer: Connecting Cellular Processes with Therapy project (QuIC-ConCePT project) from the Innovative Medicines Initiative (IMI) for partly funding the project. The funders had no role in study design, data collection and analysis, decision to publish, or preparation of the manuscript.

Appendix A. Supplementary data

Supplementary data to this article can be found online at http://dx.doi.org/10.1016/j.nucmedbio.2017.05.002.

References

[1] Shields AF, Grierson JR, Dohmen BM, Machulla HJ, Stayanoff JC, Lawhorn-Crews JM, et al. Imaging proliferation in vivo with [F-18]FLT and positron emission tomography. Nat Med 1998;4(11):1334–6.
[2] Been LB, Suurmeijer AJ, Cobben DC, Jager PL, Hoekstra HJ, Elsinga PH. [18F]FLT-PET in oncology: current status and opportunities. Eur J Nucl Med Mol Imaging 2004;31(12):1659–72.
[3] Salskov A, Tammisetti VS, Grierson J, Vesselle H. FLT: measuring tumor cell proliferation in vivo with positron emission tomography and 3′-deoxy-3′-[18F]fluorothymidine. Semin Nucl Med 2007;37(6):429–39.
[4] Bollineni VR, Kramer GM, Jansma EP, Liu Y, Oyen WJ. A systematic review on [(18)F]FLT-PET uptake as a measure of treatment response in cancer patients. Eur J Cancer 2016;55:81–97.
[5] Frings V, Yaqub M, Hoyng LL, Golla SS, Windhorst AD, Schuit RC, et al. Assessment of simplified methods to measure 18F-FLT uptake changes in EGFR-mutated non-small cell lung cancer patients undergoing EGFR tyrosine kinase inhibitor treatment. J Nucl Med 2014;55(9):1417–23.
[6] Boellaard R. Standards for PET image acquisition and quantitative data analysis. J Nucl Med 2009;50(Suppl. 1):11S–20S.
[7] Boktor RR, Walker G, Stacey R, Gledhill S, Pitman AG. Reference range for intrapatient variability in blood-pool and liver SUV for 18F-FDG PET. J Nucl Med 2013;54(5):677–82.
[8] Paquet N, Albert A, Foidart J, Hustinx R. Within-patient variability of (18)F-FDG: standardized uptake values in normal tissues. J Nucl Med 2004;45(5):784–8.
[9] Minn H, Zasadny KR, Quint LE, Wahl RL. Lung cancer: reproducibility of quantitative measurements for evaluating 2-[F-18]-fluoro-2-deoxy-D-glucose uptake at PET. Radiology 1995;196(1):167–73.
[10] Wahl RL, Zasadny K, Helvie M, Hutchins GD, Weber B, Cody R. Metabolic monitoring of breast cancer chemohormonotherapy using positron emission tomography: initial evaluation. J Clin Oncol 1993;11(11):2101–11.
[11] Wondergem MJ, Rizvi SN, Jauw Y, Hoekstra OS, Hoetjes N, van de Ven PM, et al. 18F-FDG or 3′-deoxy-3′-18F-fluorothymidine to detect transformation of follicular lymphoma. J Nucl Med 2015;56(2):216–21.
[12] de Langen AJ, Klabbers B, Lubberink M, Boellaard R, Spreeuwenberg MD, Slotman BJ, et al. Reproducibility of quantitative 18F-3′-deoxy-3′-fluorothymidine measurements using positron emission tomography. Eur J Nucl Med Mol Imaging 2009;36(3):389–95.
[13] Kenny L, Coombes RC, Vigushin DM, Al-Nahhas A, Shousha S, Aboagye EO. Imaging early changes in proliferation at 1 week post chemotherapy: a pilot study in breast cancer patients with 3′-deoxy-3′-[18F]fluorothymidine positron emission tomography. Eur J Nucl Med Mol Imaging 2007;34(9):1339–47.
[14] Zander T, Scheffler M, Nogova L, Kobe C, Engel-Riedel W, Hellmich M, et al. Early prediction of nonprogression in advanced non-small-cell lung cancer treated with erlotinib by using [(18)F]fluorodeoxyglucose and [(18)F]fluorothymidine positron emission tomography. J Clin Oncol 2011;29(13):1701–8.
[15] Wahl RL, Jacene H, Kasamon Y, Lodge MA. From RECIST to PERCIST: evolving considerations for PET response criteria in solid tumors. J Nucl Med 2009;50(Suppl. 1):122S–50S.
[16] Shankar LK, Hoffman JM, Bacharach S, Graham MM, Karp J, Lammertsma AA, et al. Consensus recommendations for the use of 18F-FDG PET as an indicator of therapeutic response in patients in National Cancer Institute trials. J Nucl Med 2006;47(6):1059–66.
[17] Boellaard R, Delgado-Bolton R, Oyen WJ, Giammarile F, Tatsch K, Eschner W, et al. FDG PET/CT: EANM procedure guidelines for tumour imaging: version 2.0. Eur J Nucl Med Mol Imaging 2015;42(2):328–54.
[18] Boellaard R, Krak NC, Hoekstra OS, Lammertsma AA. Effects of noise, image resolution, and ROI definition on the accuracy of standard uptake values: a simulation study. J Nucl Med 2004;45(9):1519–27.
[19] Krak NC, Boellaard R, Hoekstra OS, Twisk JW, Hoekstra CJ, Lammertsma AA. Effects of ROI definition and reconstruction method on quantitative outcome and applicability in a response monitoring trial. Eur J Nucl Med Mol Imaging 2005;32(3):294–301.
[20] Lodge MA, Holdhoff M, Leal JP, Bag AK, Nabors LB, Mintz A, et al. Repeatability of 18F-FLT PET in a multicenter study of patients with high-grade glioma. J Nucl Med 2017;58(3):393–8.
[21] Lubberink M, Direcks W, Emmering J, van Tinteren H, Hoekstra OS, van der Hoeven JJ, et al. Validity of simplified 3′-deoxy-3′-[18F]fluorothymidine uptake measures for monitoring response to chemotherapy in locally advanced breast cancer. Mol Imaging Biol 2012;14(6):777–82.
[22] Cheebsumon P, Velasquez LM, Hoekstra CJ, Hayes W, Kloet RW, Hoetjes NJ, et al. Measuring response to therapy using FDG PET: semi-quantitative and full kinetic analysis. Eur J Nucl Med Mol Imaging 2011;38(5):832–42.
[23] Kuhnert G, Boellaard R, Sterzer S, Kahraman D, Scheffler M, Wolf J, et al. Impact of PET/CT image reconstruction methods and liver uptake normalization strategies on quantitative image analysis. Eur J Nucl Med Mol Imaging 2016;43(2):249–58.